Exploring Cosmic Dawn with the Hydrogen Epoch of Reionization Array

Adélie Gorce

e-mail: adelie.gorce@mcgill.ca

McGill Space Institute & Department of Physics, McGill University, Montreal, QC, Canada

Presented at the 4th World Summit on Exploring the Dark Side of the Universe
La Réunion, November 7-11 2022

Abstract

One of the main challenges of modern cosmology resides in the observation of the 21 cm signal from neutral Hydrogen. The 21 cm signal has the potential of unveiling the nature of the first stars and the timeline of their birth, through their ionisation of the neutral IGM during the Epoch of Reionisation (EoR). Despite the efforts of many experiments around the globe, extremely bright foregrounds, low signal to noise, and instrument systematics have prevented astronomers from observing this high-redshift signal.

In this talk, I will present the results of the Hydrogen Epoch of Reionization Array (HERA), a low-frequency radio interferometer located in the Karoo desert, in South Africa, and an official precursor to the SKA. I will describe the approach chosen to mitigate foregrounds and the methods developed to deconvolve instrument characteristics, such as the chromaticity of the beam, to reach detection. HERA has recently published the lowest upper limits on the high-redshift power spectrum of the 21 cm signal to date, allowing to constrain, for the first time, the properties of the high-redshift Universe. I will describe how we obtained these results and their implications in terms of cosmology and the astrophysics of the IGM. Finally, I will outline the future of HERA and what outstanding results we can expect from the instrument.

1 Introduction

The first light sources in the Universe appear at a time called Cosmic Dawn, a few hundred million years after recombination and the emission of the Cosmic Microwave Background (CMB). Progressively, the radiation emitted by these sources ionises the neutral atoms of the surrounding intergalactic medium (IGM). This time, called the Epoch of Reionisation, is a billion-year-long missing piece in our knowledge of cosmic history. The chronology and the morphology of cosmic reionisation are crucial sources of information about the nature of the first astronomical objects, of the young Universe, and about the formation of the first galaxies. As illustrated in Figure 1, the physical properties of the

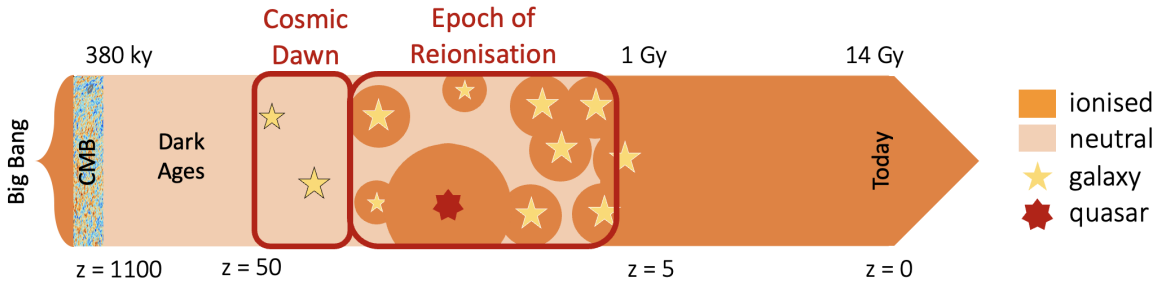

Figure 1: Figure illustrating the birth of the first light sources during Cosmic Dawn and their ionisation of the intergalactic medium during the Epoch of Reionisation.

source impact the shape and growth of the surrounding ionised bubble it forms, with, e.g., quasars expected to form larger and rounder bubbles than galaxies.

If reionisation is largely unknown, we already have some clues about its history. The spectra of distant quasars tell us that reionisation was likely over by a redshift $z = 6$ [1], the density of high-redshift galaxies seems sufficient to ionise the entirety of the IGM without the help of exotic sources [2], and the CMB optical depth is compatible with a reionisation halfway through at $z = 6.5$ [3, 4]. However, these results are based on strong hypotheses made about the early Universe and are not sufficient to give a clear picture of the Epoch of Reionisation [5].

2 Measuring the 21 cm power spectrum at $z > 5$

A potential solution is the observation of the 21 cm signal emitted by neutral hydrogen atoms before they got ionised by early galaxies, a direct tracer of cosmic reionisation. Indeed, the brightness temperature of this signal is proportional to the density and ionisation level of the intergalactic gas. The photons emitted with an exact wavelength of 21 cm are redshifted to larger wavelengths, with the potential of mapping the distribution of neutral hydrogen in the Universe at any given time.

Many low-frequency radio experiments target this signal, for which no observation has yet been confirmed [6, 7]. In this talk, we focus on the measurement of the power spectrum of the spatial fluctuations of the 21 cm signal from $z > 5$, which contains information on both the chronology and the morphology of reionisation. This measurement is a world-wide effort involving many international collaborations around the word such as, e.g., the Giant Metre Wave Radio Telescope [GMRT, 8] in India, the Low Frequency Array [LOFAR, 9] in the Netherlands, the Murchison Widefield Array [MWA, 10] in Australia and the Hydrogen Epoch of Reionization Array [HERA, 11] in South Africa, on which we will focus today.

2.1 The Hydrogen Epoch of Reionization Array

HERA is a radio interferometer made of (as of today) about 100 14m parabolic dishes, some of which are shown in Figure 2. It observes a 10-degree stripe at fixed declination in the Southern hemisphere, with a bandwidth covering frequencies ranging from 100 to 200 MHz, or redshifts $6 \leq$

Figure 2: Picture of HERA taken on-site in January 2017. Reproduced from [12].

$z \leq 13$. In radio interferometry, one measures a visibility V_{ij} between two antennae i and j separated by a length b_{ij} called baseline. This visibility measured at a frequency ν writes

$$V_{ij}(\nu) = \int B_{ij}(\hat{\mathbf{r}}, \nu) I(\hat{\mathbf{r}}, \nu) \exp\left[-2\pi i \frac{\nu}{c} \mathbf{b}_{ij} \cdot \hat{\mathbf{r}}\right] d\Omega, \tag{1}$$

where B_{ij} is the beam of the instrument and I is the signal intensity. From this equation, is it clear than the baseline length b_{ij} is analogous to a Fourier dual of the sky angle. For this reason, dense arrays will measure large-scale fluctuations on the sky, whilst wide arrays, such as HERA, measure small-scale fluctuations.

One of the main difficulties with observing the 21 cm from the Epoch of Reionisation lies in extremely bright foregrounds, about 4 to 5 orders of magnitude brighter than the cosmological signal. However, in contrast to the cosmological signal, these foregrounds are spectrally smooth, such that we can separate these two components in Fourier space. This is the strategy chosen by HERA: maximising sensitivity and targeting observations in a region of Fourier space called the 'Eor window' where the cosmological signal dominates, despite the chromaticity of the instrument introducing foregrounds leakage outside of their intrinsic spectral region [13]. To this end, to facilitate calibration, and to improve the signal-to-noise ratio, HERA is a highly redundant hexagonal array, that is the antennae are arranged such that the same baseline $\boldsymbol{b}_{ij}$ is sampled many times [11].

2.2 The latest HERA results

In [12], the HERA collaboration presents world-leading upper limits on the 21 cm power spectrum at $z = 7.9$ and $z = 10.4$, with one full season of data (94 nights) and 42 antennae. In Figure 3, we present the limits obtained along Band 2 ($z = 7.9$), and the corresponding window functions. These limits are over a factor two lower than our previous results [14] and allow us to put constraints on the early Universe.

To interpret these upper limits theoretically, we confront different types of simulations to the data, and fit for their parameters (see [15] for details). As illustrated in Figure 4, for all theory models, we

find that the posterior for the power spectrum tightens substantially, and that the IGM was heated by $z = 10.4$, likely by high-mass X-ray binaries.

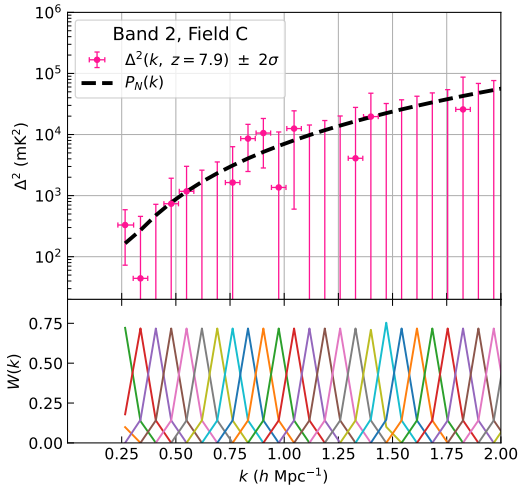

Figure 3: *Upper panel:* Dimensionless 21 cm power spectrum measured by HERA at $z = 7.9$ for one field (in pink, see [12] for details), compared to the noise power spectrum (black dashed line). *Lower panel:* Corresponding window functions (horizontal error bars).

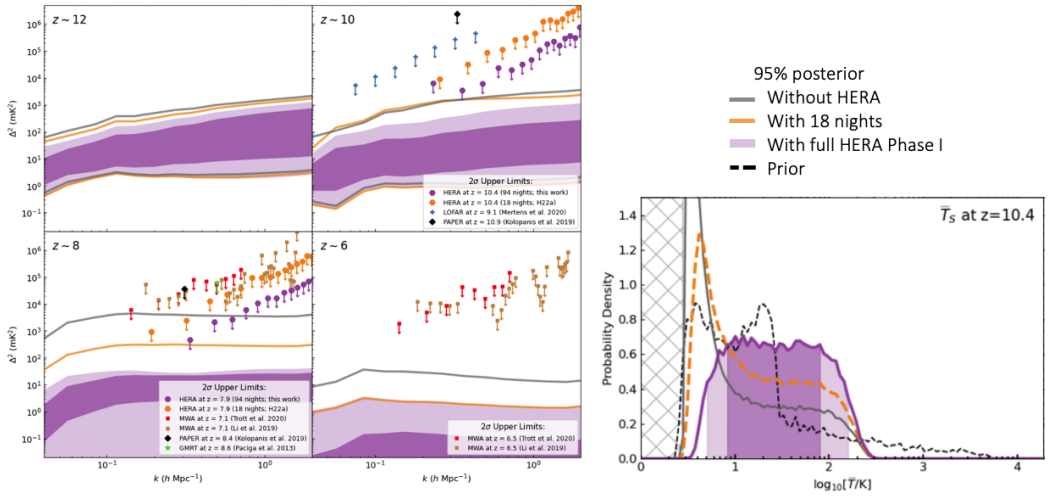

Figure 4: Posterior distributions of the 21 cm power spectrum obtained with 21CMMC [16] at different redshifts, including the two probed by HERA (left panel) and of the mean spin temperature in the IGM at $z = 10.4$ (right panel). Inferences are compared when using non-HERA astrophysical data sets, when adding partial HERA data, and when adding the full first season of HERA data. On the left panel, different data points correspond to different experiments, the HERA results correspond to the purple hexagons. On the right panel, the hashed region indicates temperatures below the adiabatic cooling limit.

2.3 Building confidence in and understanding the HERA results

In [17], we introduce an end-to-end validation pipeline, helping us build confidence in our results. We simulate visibilities including a mock cosmological signal – a Gaussian random field whose power power spectrum goes as $P(k) \propto k^{-2}$, and foregrounds. These clean visibilities are then contaminated with instrumental effects and systematics such as thermal noise, antenna gains, cross-coupling, and cable reflections. Data sets with different components are run through the same analysis pipeline as the observations. We are able to recover the cosmological signal in the simulated data set, outside of the foreground-dominated ('foreground wedge', $k \gtrsim 0.15\ h\mathrm{Mpc}^{-1}$) and of the noise-dominated ($k \lesssim 0.6\, h\mathrm{Mpc}^{-1}$) regions. We refer the interested reader to [17] for more details.

We also build our understanding of the measurements by studying systematics, namely with systematics chromatography [18] and getting a precise estimate of the window functions of the instrument [19]. Indeed, the power measured at one Fourier mode k receives contributions from neighbouring modes, which can be especially problematic for data points located close to the foreground wedge, as shown with various test cases in [19]. These window functions, illustrated in the bottom panel of Figure 3 in spherical space and in Figure 5 in cylindrical space, are the key to know precisely how the true cosmological power spectrum and what is measured by the instrument differ. They will be impacted by instrument characteristics and data analysis choices. Namely, long baselines will correspond to wider window functions, facilitating foreground leakage, whilst the choice of bandwidth and frequency taper can help narrowing them down.

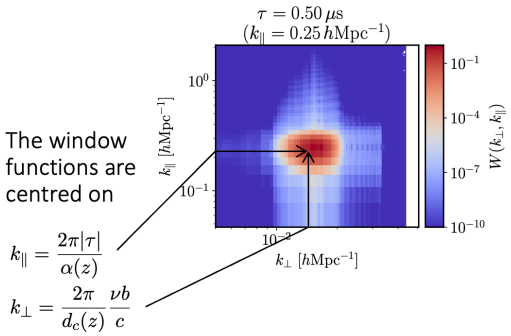

Figure 5: *Upper panel:* Dimensionless 21 cm power spectrum measured by HERA at $z = 7.9$ for one field (in pink, see [12] for details), compared to the noise power spectrum (black dashed line). *Lower panel:* Corresponding window functions (horizontal error bars).

3 Conclusions

With a full season of data and conservative analysis techniques, the HERA collaboration has been able to bring their upper limits down by more than a factor two to obtain world-leading results and tighten our power spectrum posteriors, ruling out cold reionisation scenarios. However, results remain at the thermal noise limit.

Recent improvements made to the array will further lower these upper limits, thanks to a collecting area multiplied by five. With new feeds, we also extended our bandwidth to $50 < \nu/\mathrm{MHz} < 250$,

reaching redshifts as far as $z = 29$ and as low as $z = 4.7$. The new frequencies covered will allow us to confirm or infirm the global 21 cm signal observation claimed by EDGES [6]. Once the full array will be deployed, with its 350 antennae, we will be able to constrain the reionisation history at $z \pm 0.1$ [20].

Acknowledgements

This material is based upon work supported by the National Science Foundation under Grant Nos. 1636646 and 1836019 and institutional support from the HERA collaboration partners. This research is funded in part by the Gordon and Betty Moore Foundation through Grant GBMF5212 to the Massachusetts Institute of Technology. HERA is hosted by the South African Radio Astronomy Observatory, which is a facility of the National Research Foundation, an agency of the Department of Science and Innovation. My work is supported by the McGill Astrophysics Fellowship funded by the Trottier Chair in Astrophysics as well as the Canada 150 Programme. I also acknowledge support by the Canadian Institute for Advanced Research (CIFAR) Azrieli Global Scholars program.

References

[1] X. Fan, M. A. Strauss, R. H. Becker, et al., *Constraining the Evolution of the Ionizing Background and the Epoch of Reionization with z = 6 Quasars. II. A Sample of 19 Quasars*, *ApJ* **132** (July, 2006) 117–136, [astro-ph/0512082].

[2] B. E. Robertson, R. S. Ellis, S. R. Furlanetto, and J. S. Dunlop, *Cosmic Reionization and Early Star-forming Galaxies: A Joint Analysis of New Constraints from Planck and the Hubble Space Telescope*, *ApJ Letters* **802** (Apr., 2015) L19, [arXiv:1502.02024].

[3] Planck Collaboration et al., *Planck intermediate results. XLVII. Planck constraints on reionization history*, *A&A* **596** (Dec., 2016) A108, [arXiv:1605.03507].

[4] A. Gorce, M. Douspis, and L. Salvati, *Retrieving cosmological information from small-scale CMB foregrounds. II. The kinetic Sunyaev Zel'dovich effect*, *A&A* **662** (June, 2022) A122, [arXiv:2202.08698].

[5] A. Gorce, M. Douspis, N. Aghanim, and M. Langer, *Observational constraints on key-parameters of cosmic reionisation history*, *A&A* **616** (Aug, 2018) A113, [arXiv:1710.04152].

[6] J. D. Bowman, A. E. E. Rogers, R. A. Monsalve, T. J. Mozdzen, and N. Mahesh, *An absorption profile centred at 78 megahertz in the sky-averaged spectrum*, *Nature* **555** (Mar., 2018) 67–70, [arXiv:1810.05912].

[7] S. Singh, N. T. Jishnu, R. Subrahmanyan, N. Udaya Shankar, B. S. Girish, A. Raghunathan, R. Somashekar, K. S. Srivani, and M. Sathyanarayana Rao, *On the detection of a cosmic dawn signal in the radio background*, *Nature Astronomy* **6** (Feb., 2022) 607–617, [arXiv:2112.06778].

[8] S. Ananthakrishnan, *The Giant Meterwave Radio Telescope / GMRT*, *Journal of Astrophysics and Astronomy Supplement* **16** (Jan., 1995) 427.

[9] M. P. van Haarlem, M. W. Wise, A. W. Gunst, G. Heald, J. P. McKean, J. W. T. Hessels, A. G. de Bruyn, R. Nijboer, J. Swinbank, R. Fallows, and et al., *LOFAR: The LOw-Frequency ARray*, *A&A* **556** (Aug., 2013) A2, [arXiv:1305.3550].

[10] S. J. Tingay, R. Goeke, J. D. Bowman, D. Emrich, S. M. Ord, et al., *The Murchison Widefield Array: The Square Kilometre Array Precursor at Low Radio Frequencies*, *PASA* **30** (Jan., 2013) e007, [arXiv:1206.6945].

[11] D. R. DeBoer, A. R. Parsons, J. E. Aguirre, P. Alexander, et al., *Hydrogen Epoch of Reionization Array (HERA)*, *PASP* **129** (Apr., 2017) 045001, [arXiv:1606.07473].

[12] T. H. Collaboration, *Improved Constraints on the 21 cm EoR Power Spectrum and the X-Ray Heating of the IGM with HERA Phase I Observations*, *arXiv e-prints* (Oct., 2022) arXiv:2210.04912, [arXiv:2210.04912].

[13] A. Liu, A. R. Parsons, and C. M. Trott, *Epoch of reionization window. I. Mathematical formalism*, *Phys. Rev. D* **90** (Jul, 2014) 023018, [arXiv:1404.2596].

[14] The HERA Collaboration, *First Results from HERA Phase I: Upper Limits on the Epoch of Reionization 21 cm Power Spectrum*, *ApJ* **925** (Feb., 2022) 221.

[15] The HERA Collaboration, *HERA Phase I Limits on the Cosmic 21-cm Signal: Constraints on Astrophysics and Cosmology During the Epoch of Reionization*, *arXiv e-prints* (Aug., 2021) arXiv:2108.07282, [arXiv:2108.07282].

[16] B. Greig and A. Mesinger, *21CMMC: an MCMC analysis tool enabling astrophysical parameter studies of the cosmic 21 cm signal*, *MNRAS* **449** (Jun, 2015) 4246–4263, [arXiv:1501.06576].

[17] J. E. Aguirre, S. G. Murray, R. Pascua, Z. E. Martinot, et al., *Validation of the HERA Phase I Epoch of Reionization 21 cm Power Spectrum Software Pipeline*, *ApJ* **924** (Jan., 2022) 85, [arXiv:2104.09547].

[18] N. S. Kern, A. R. Parsons, J. S. Dillon, et al., *Mitigating Internal Instrument Coupling for 21 cm Cosmology. II. A Method Demonstration with the Hydrogen Epoch of Reionization Array*, *ApJ* **888** (Jan., 2020) 70, [arXiv:1909.11733].

[19] A. Gorce, S. Ganjam, A. Liu, S. G. Murray, and the HERA collaboration, *Impact of instrument and data characteristics in the interferometric reconstruction of the 21cm power spectrum*, *arXiv e-prints* (Oct., 2022) arXiv:2210.03721, [arXiv:2210.03721].

[20] A. Liu and A. R. Parsons, *Constraining cosmology and ionization history with combined 21 cm power spectrum and global signal measurements*, *MNRAS* **457** (Apr., 2016) 1864–1877, [arXiv:1510.08815].